A near-optimal rule-based energy management strategy for medium duty hybrid truck

Riccardo Biasini*

Tesla Motors Inc.,
Palo Alto, CA, 94304, USA
E-mail: riccardo.biasini@gmail.com
*Corresponding author

Simona Onori

Centre for Automotive Research,
The Ohio State University,
Columbus, OH, 43212, USA
E-mail: onori.1@osu.edu

Giorgio Rizzoni

Centre for Automotive Research,
The Ohio State University,
Columbus, OH, 43212, USA
and
Mechanical and Aerospace Engineering Department,
The Ohio State University,
Columbus, OH, 43212, USA
E-mail: rizzoni.1@osu.edu

Abstract: This paper covers the design and implementation of a rule-based energy management strategy for a medium duty hybrid truck. In this paper, a procedure for the design of a near-optimal energy management strategy is presented. The procedure utilises the dynamic programming (DP) algorithm to find the optimal control strategy that minimises the fuel consumption over a given driving mission. Through the analysis of the behaviour of DP control actions, near-optimal rules are extracted and tuned to design a rule-based strategy for charge sustaining operation which, unlike DP control signals, is implementable on-board of the vehicle. Drivability metrics such as frequent clutching and engine on/off behaviour are also included in the control design based on the implementation of the DP under different drivability scenarios.

The performance of the proposed energy management control strategy is studied by using a proposed longitudinal vehicle model of a pre-transmission parallel medium duty hybrid truck with a clutch. The proposed near-optimal rule-based strategy, benchmarked against the optimal DP solution, shows performance within 3% of the global optimal one.

Keywords: hybrid truck; hybrid electric vehicle; HEV; dynamic programming; powertrain modelling; rule-based control strategy.

Biographical notes: Riccardo Biasini obtained his BS and MS degrees in Aerospace Engineering and Automotive Engineering, from University of Pisa, Italy in 2008 and 2010, respectively. After internships at Fermi National Laboratory Accelerator, Dallara Automobili, and Centre for Automotive Research (the Ohio State University), he started working as a System Designer and Architect Engineer at Tesla Motors, USA, in 2011. His main area of interest is powertrain modelling for EVs.

Simona Onori is a Research Scientist at the Ohio State University Center for Automotive Research and a Lecturer at the MAE Department, OSU. She received her Laurea degree, Summa Cum Laude in ECE from University of Rome 'Tor Vergata', MS in EE from University of New Mexico, and PhD in Control Engineering from University of Rome 'Tor Vergata' in 2003, 2004 and 2007, respectively. Her research is in control system theory and applications. She is currently focusing on model-based control design in advanced propulsion systems, energy management optimisation in hybrid vehicles, fault diagnosis and prognosis for automotive applications.

Giorgio Rizzoni is the Ford Motor Company Chair in Electromechanical Systems. He is a Professor of Mechanical and Aerospace Engineering and of Electrical and Computer Engineering, and Director of the Center for Automotive Research (an interdisciplinary research centre supporting 30 full-time staff and 70 graduate students) at the Ohio State University. His research interests include dynamics, control and diagnosis of automotive systems, with emphasis on hybrid and electric vehicles, and on energy conversion and storage systems. He received his BS, MS and PhD degrees in Electrical and Computer Engineering from the University of Michigan. He is also a Fellow of IEEE and SAE.

1 Introduction

With the demand for greener cars and the reduction of fuel consumption optimal use of the available sources of energy in a vehicle is required. This translates in complex powertrains and vehicle architectures and control strategies that must be implemented to remain competitive in the market. Hybrid electric vehicles (HEVs) represent a powerful means to save fuel and reduce CO_2 emissions. Their performance strongly depends on the energy management strategy onboard of the vehicle. The HEV control problem involves the determination of the optimal power flow, namely, the power split between the internal combustion engine (ICE) and the electric motors (EMs) (Salman et al., 2000; Sciarretta and Guzzella, 2007). Finding the sequence of optimal power split at each instant to minimise the fuel consumption over a driving cycle is the aim of the energy management control for HEVs. In general, the energy management control is implemented in the vehicle-level control system that can coordinate the overall hybrid powertrain to satisfy certain performance target such as fuel economy, emission reduction, etc. Its commands become then the set-points for the servo-loop control systems, which operate at a much

higher frequency. The servo-loop control systems can be designed for different goals, such as improved drivability, while ensuring the set-points commanded by the main loop controller are achieved reliably.

Several strategies have been proposed in literature to solve the HEV energy management problem (see, for example, the overview in Sciarretta and Guzzella, 2007). The methods are classified into two main groups: optimal control-based methods and heuristics strategies.

1   *Optimal control-based methods*. In this group we find both global optimisation and instantaneous optimisation methods based on the optimal control tools (Lewis and Syrmos, 1995). Both classes of methods can guarantee global optimal solutions assuming the knowledge of the entire driving cycle. The DP (Brahma et al., 2000), the Pontryagin's minimum principle (PMP) (Cipollone and Sciarretta, 2006) and equivalent consumption minimisation strategy (ECMS) (Paganelli et al., 2001; Serrao et al., 2011), belong to this class of methods as well as other numerical search methods such as, e.g., genetic algorithms (Piccolo et al., 2001). The main limitation of these methods is in their impossibility of being implementable in real time as their solutions rely on future unknown information.

2   *Heuristic methods*. These methods do not involve explicit optimisation; instead, the energy management is implemented through heuristic rules. Rule-based control (Ayalew and Molla, 2011; Jalil et al., 1997) and fuzzy logic (Salman et al., 2000) belong to this category. These strategies are computationally efficient, requiring lower computational load than optimal control-based methods. However, they may fail to fully exploit the potential of the hybrid electric architecture due to the lack of formal optimisation.

In this paper, we apply the DP technique to solve the optimal energy management problem for a hybrid electric truck. The optimal power management solution over a driving cycle is obtained by minimising a defined cost function in terms of overall fuel consumption. Although the DP control actions are not implementable they are, on the other hand, a good design tool to analyse, assess, and adjust other control strategies. The behaviour of the DP is studied to extract implementable rules and to design a rule-based strategy whose performance are shown, in simulation, to be very close to the DP solution.

The paper is organised as follows: in Section 2 the powertrain architecture of a medium duty hybrid truck is introduced and the role of the hybrid controller in HEV is discussed; in Section 3 the energy management problem for charge sustaining HEVs is introduced and the mathematical model of the hybrid electric truck is described in Section 4. Section 5 describes the dynamic programming (DP) algorithm and the different scenarios the DP was solved in this study. Section 6 reports on simulation results obtained from the different scenarios defined in Section 5. In Section 7 the rule-based control strategy is designed by extracting rules from the DP solutions. Moreover, the calibration procedure for tuning the RB control law and simulation results are presented. Finally, conclusions are presented in Section 8.

2 The role of hybrid controller in HEV

The energy management problem is solved in this paper for the pre-transmission parallel architecture represented in Figure 1. The power flow between the different components (the arrowheads denote the positive power sign convention) is illustrated. The main specifications of the powertrain components are reported in Table 1.

Figure 1 Parallel architecture and power flow diagram (see online version for colours)
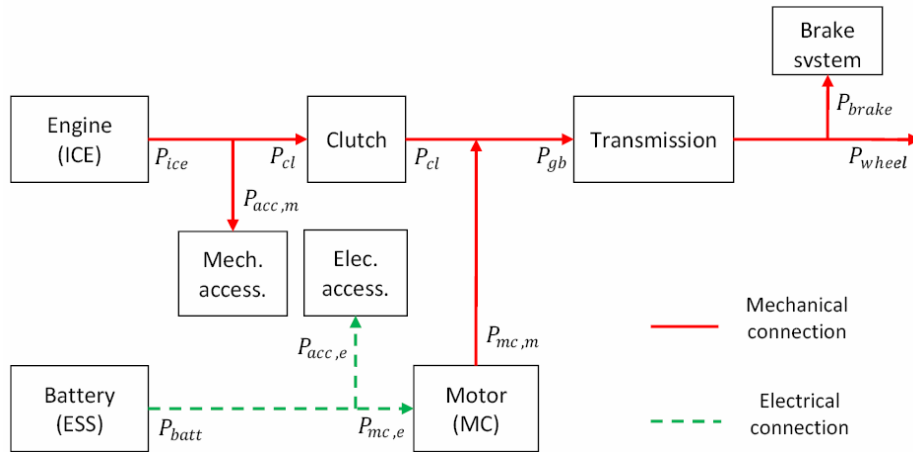
Table 1 Medium duty hybrid truck specifications

Frontal area	8 m^2
Diesel engine	6.7 L; 194 kW
Electric motor	100 kW (continuous)
	200 kW (peak)
Battery	Cell capacity: 6 Ah
	175 series cells
	2 par modules
	Battery pack capacity: 12 Ah
	Max power : 200 kW
Mechanical accessory	4 kW
Electrical accessory	7 kW

The ICE and the EM supply the requested power at the wheel allowing the possibility to recharge or deplete the battery, within a fixed range of state-of-charge (*SOC*). A clutch can be disengaged to disconnect the ICE from the powertrain: in this configuration the electric motor provides all the power during traction while the ICE can be turned off if requested.

The energy management problem is cast into an optimisation problem where the mass of fuel is being minimised over a driving mission subject to the following constraints.

- charge-sustainability: the battery SOC at the beginning and the end of the trip should be equal

- drivability constraints: at each instant, the total torque output of the powertrain should be equal to the driver's demand

- actuator limitations: at each instant, the output of each machine in the powertrain (engine and motor) cannot exceed its maximum torque/power rating; similarly, the total battery power must remain within the acceptable limits in both charge and discharge operations.

The general structure of hybrid controller is shown in Figure 2. The *supervisory module* decides upon the available modes the powertrain should operate (EV or parallel), whereas the *energy management module* determines the optimal power split between the on-board energy sources.

Figure 2   Two layer hybrid control structure
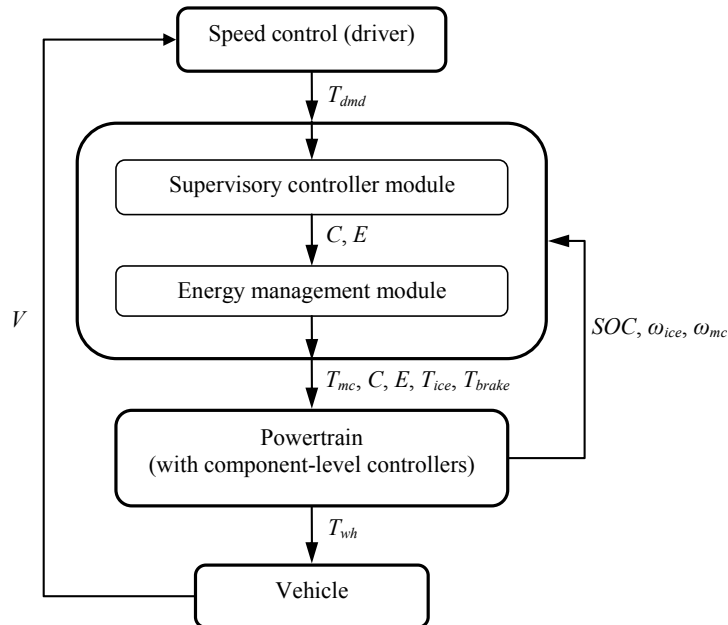
In the vehicle architecture we distinguish discrete and continuous variables. The status of the clutch (locked or unlocked) and the status of the engine (on or off) are discrete control variables that determine the operating mode of the powertrain, whereas the torque of the electric machine is a continuous control variable which determines, at each sampling instant, how the power request is shared between the actuators.

Thus, the control vector is given by:

$$u = \{T_{mc}, C, E\},$$

where T_{mc} is the motor torque, C is the clutch status ($C = 1$ for clutch closed, $C = 0$ for clutch open), and E is the engine status ($E = 1$ when the engine is on, $E = 0$ when it is off). The value of the variables C and E is determined at the supervisory controller level,

while T_{mc} is determined at the energy management level, meeting the constraints during vehicle operation.

The transmission gear index is chosen by the transmission controller, which is assumed to be external to the energy management and supervisory controller; therefore, the gear index is treated as known external input in this context. The vehicle velocity, the rotational speed of the ICE and the electric machine and the driver torque demand are also external inputs of the two-layer hybrid control and they determine the gear index.

The aim of this paper is to develop a rule-based strategy according to the two-layer structure of Figure 2. To achieve this goal we follow the approach proposed in Bianchi et al. (2011) which relies on first finding the global optimal solution of the optimisation problem by means of the DP solution (as in Lin et al., 2003) and then, from this, extracting static rules to be implemented in a two-layer controller to reproduce the optimal behaviour.

3 Energy management problem for HEV

The optimal energy management problem consists in finding the control function $u(t)$ that leads to the minimisation of the performance index, defined as:

$$J\big(u(t)\big) = \int_{t_0}^{t_f} \dot{m}_f\big(u(t)\big) dt,$$

where t is time, $u(t)$ is the control action, $t_f - t_0$, is the optimisation horizon, $\dot{m}_f(u(t))$ is the instantaneous cost function, i.e., the fuel consumption rate.

With a quasi-static engine model, the fuel consumption is only a function of the engine torque, $T_{ice}(t)$ and the speed $\omega_{ice}(t)$. The dependence of these variables on the driver's torque demand $T_{dmd}(t)$, the control $T_{mc}(t)$, and the vehicle speed $V(t)$, allows us to express the fuel consumption as $\dot{m}_f(T_{mc}(t), T_{dmd}(t), V(t))$.

The vehicle speed and the torque demand are considered as external inputs; the dynamics of the powertrain components are neglected [as being much faster than the SOC dynamics and not affecting the vehicle energy balance significantly (Sendur et al., 2003)]. The constraints to which the optimisation is subject to are listed below:

a   *System dynamics*. In HEVs, the system dynamics are represented by the evolution of the state-of-charge according to:

$$\dot{SOC}(t) = -\frac{I(t)}{Q_{batt}}$$

where $I(t)$ is the current in and out of the battery (positive during discharge).

b   *Initial state value*. The system state at the beginning of the optimisation horizon assumes the initial value $SOC_0 = SOC(0) = 0.68$.

c   *Terminal state value*. The terminal value of the state must satisfy the constraint $SOC_f = SOC(t_f) = 0.68$.

Note: Conditions b and c define the charge-sustaining constraint assumed in this work.

d   *Instantaneous state limitations*. At each time $t \in [t_0, t_f]$, the state of charge must remain within lower and upper bounds:

$$0.5 \leq SOC(t) \leq 0.8$$

e   *Instantaneous control limitations*. At each time, the control variable $u(t)$ must be in the set of given admissible controls. The definition of the admissible control set is specific to each architecture: The general guidelines are that the controls must be such that the torque or power delivered by each machine does not exceed their intrinsic limitations, while at the same time, the total torque or power demand at the wheel is satisfied (to the highest degree possible).

At this point, the optimal control problem is completely defined. The following sections show how the optimisation problem can be solved by means of DP to obtain the optimal global solution, once the driving cycle is known. In Section 5, results from the DP algorithm are analysed and studied to extract meaningful characteristic of the optimal solution that can be reproduced and synthesise within a rule-based strategy framework.

4   Medium duty hybrid truck model

In this paper a backward simulator (Musardo et al., 2005) of the medium duty hybrid truck is developed to first find the global solution from the DP algorithm, and then to implement the rule-based strategy derived from it. The net tractive force is calculated given the velocity, payload, and grade profile, along with the vehicle characteristics. A large number of combinations of actuators power (i.e., motor, engine, brake system) can satisfy the driver demand, but only one combination at each time gives the optimal control; the fuel consumption is evaluated as a consequence of the decision made by the optimal controller.

   The backward simulator is a quasi-static model: all the dynamics are neglected and each component is represented through stationary maps experimentally measured; in particular, the clutch and the engine cranking transients are neglected.

4.1   Powertrain model

Starting from the driving cycle inputs, the traction force at the wheel that the powertrain (including the brake system) has to generate in order to satisfy the dynamic constraints is given by:

$$F_w = F_i + F_r + F_a + F_g. \tag{1}$$

Each term in the above equation is computed as follows:

•   *Rolling resistance:*

$$F_r = c_r Mg \cos \alpha. \tag{2}$$

where g is the gravity acceleration, α is the road slope, M is the vehicle mass and c_r is the rolling resistance coefficient which, in principle, is a function of vehicle speed, tire pressure, external temperature, etc. In most cases, c_r is assumed to be a cubic polynomial function of the speed V:

$$c_r = c_0 + c_1 V + c_2 V^2 + c_3 V^3. \tag{3}$$

- *Aerodynamic resistance:*

$$F_\alpha = \frac{1}{2} \rho_{air} A C_d V^2, \tag{4}$$

where ρ_{air} is the air density, A the vehicle frontal area, C_d the aerodynamic drag coefficient.

- *Road slope:*

$$F_g = Mg \sin \alpha, \tag{5}$$

where α is the slope angle of the road.

- *Inertia:*

$$F_i = M_{eq} \frac{dV}{dt}, \tag{6}$$

where M_{eq} is the equivalent mass that takes in account all the inertia of the driveline component and can be expressed as:

$$M_{eq} = M + J_w \frac{1}{R^2} + J_{ice} \frac{\tau_{gb}^2 \tau_d^2}{R^2}, \tag{7}$$

where M is the vehicle mass, J_w is the overall inertia of the four wheels (which includes tires, brake discs, half shafts), J_{ice} is the engine inertia, R is wheel radius, τ_{gb} is the transmission gear ratio and $\tau_d \tau$ is the final drive gear ratio.

Neglecting for this instance the wheel inertia, equation (8) considers the wheel equilibrium to evaluate the gearbox input torque, T_{gb}:

$$F_w R = T_{gb} \eta_{gb}^{sign(T_{gb})} \eta_d^{sign(T_{gb})} \tau_{gb} \tau_d - T_b, \tag{8}$$

where T_b is the total braking torque applied by the friction braking system, η_{gb} and η_d are the efficiencies of the gearbox and the final drive, respectively.

All the vehicle parameters used in the previous equations are supposed to be known by the control strategy; the driver's wheel torque demand (determined by the accelerator pedal position) is the request that the hybrid propulsion system must satisfy through the application of an adequate T_{gb} and the braking torque T_{brake}. The way this is done depends on the operating mode of the vehicle, as explained below.

- *EV mode engine off:* the mechanical accessories, which are belted to the engine shaft, are not powered. The vehicle is then powered only by the motor, which is electrically connected to the battery.

  In this case there are no degrees of freedom and the EM torque is given by:

$$T_{gb} = T_{mc}, \quad T_{ice} = 0. \tag{9}$$

  The engine speed is zero and the motor speed is the gearbox speed.

$$\omega_{mc} = \omega_{gb}, \quad \omega_{ice} = 0. \tag{10}$$

- *EV mode engine on:* the engine is on at idle speed; mechanical accessories are belted to the engine shaft are powered by the engine. The vehicle is driven only by the motor, which is powered by the battery alone. In this case there are no degrees of freedom and the EM torque is given by the gearbox torque, while the engine torque is required for the mechanical accessories:

$$T_{gb} = T_{mc}, \quad T_{ice} = \frac{P_{accmech}}{\omega_{ice}}. \tag{11}$$

The engine speed is the idle speed, while the motor is coupled with the gearbox.

$$\omega_{mc} = \omega_{gb}, \quad \omega_{ice} = \omega_{idl}. \tag{12}$$

- *Parallel mode:* if the system is in the parallel configuration the clutch is engaged and both the engine and the EM are connected to the powertrain. In this configuration the sum of the EM and engine torques is equal to the total demanded torque, thus the torque at the gearbox is given by:

$$T_{gb} = T_{mc} + T_{eng} - T_{accmech} \tag{13}$$

$T_{accmech}$ is the torque absorbed by the mechanical accessories and can be calculated as follow:

$$T_{accmech} = \frac{P_{accmech}}{\omega_{eng}} \tag{14}$$

The engine speed and the motor speed are equal since devices are coupled by the clutch before at input of the gearbox:

$$\omega_{eng} = \omega_{mc} = \omega_{gb} \tag{15}$$

The battery power P_{batt} is a function of the electrical accessory power $P_{accelec}$ and EM power P_{em}.

$$P_{batt} \eta_{batt}^{sign(P_{batt})} = P_{mc,e} + P_{accelec} \tag{16}$$

The braking torque is considered only if the negative torques coming from the engine and the EM are not enough to satisfy the requested torque.

if $\quad T_{gb} + T_{accmech} \leq T_{mc,min} + T_{ice,min} \quad$ then

$$T_b = \left(T_{ice,min} + T_{mc,min} - T_{accmech} \eta_{gb}^{sign(T_{gb})} \eta_{fd}^{sign(T_{gb})} \tau_{gear} \tau_{fd} - T_{wheel} \right) \tag{17}$$

otherwise $\quad T_b = 0$

For the purpose of implementing an energy-based backward simulator, a 0th order model of the battery is used to compute the state of charge variation as a function of the power at the terminals and of the circuit parameters.

The validation of the backward model was conducted against the PSAT detailed model[1] of the pre-transmission parallel vehicle. A sampling time of 0.1 s was used to run both models. The cumulative errors on fuel consumption and on the final SOC

were 0.4% and 0.8%, respectively (Figure 3). A zoom on the dynamics of the engine torque and battery current is shown in Figure 4.

Figure 3 Macro validation of the backward model (red) against PSAT model (blue): (starting from the top) driving cycle velocity; fuel consumed; SOC profile (see online version for colours)
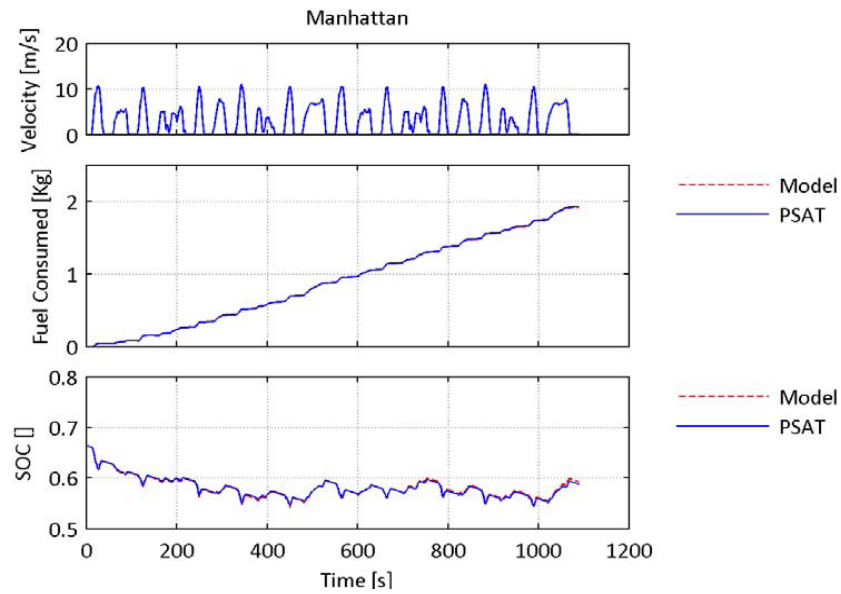
Figure 4 Transient dynamics validation of the backward model (red) against PSAT model (blue): (starting from the top) driving cycle velocity; engine torque; battery current (see online version for colours)
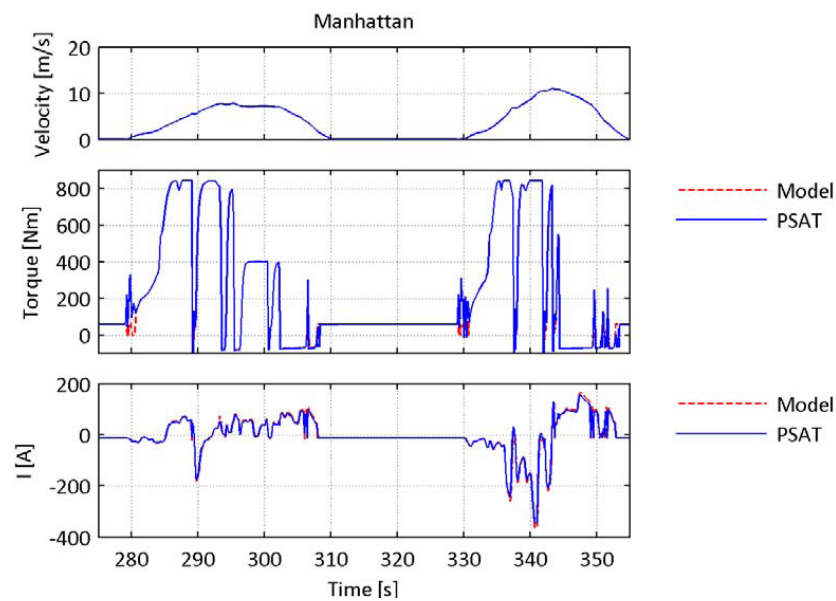
5   Dynamic programming

DP generates a numerical solution to the optimal control problem defined in Section 3 based on Bellman's principle of optimality (Salman et al., 2000). In order to apply DP for the problem at hand, the system dynamics and the control domain are written in a discrete-time form. To implement the DP algorithm on described hybrid architecture, an open-source MATLAB code developed at ETH-Zurich (Sundström and Guzzella, 2009) was exploited. This function solves discrete-time optimal control problems using Bellman's DP algorithm. The user has to provide the number of controls that need to be optimised, the states of the system that have to be monitored and the limits for each of them. Then the code pre-processes this information in order to arrange all the possible input values into multi-dimensional matrices. The sequence of control actions are applied, step-by-step, to a backward vehicle model that generates a grid of possible SOC values, each corresponding to a certain pattern of control inputs.

In this work, the DP has been run under three different scenarios:

1   standard with no drivability constraints

2   incorporating drivability constraints by means of an energy cost associated to the engine on/off (to limit continuous engine on-off on operations)

3   incorporating drivability constraints by means of an energy cost associated to with the clutch timing to limit continuous and repeated clutch on-off switching.

The three scenarios are detailed below.

5.1   DP with no constraints

The DP algorithm was run to solve the standard optimisation problem, where the only state variable is the state of charge. In this scenario, continuous switches of the engine off-engine-on operation are observed as well as continuous engagement and disengagement of the clutch, which compromise the overall drivability. To address this issue, the DP code was modified in order to discourage the continuous engine-off/engine-on transitions and to refrain the clutch to change continuously its status in the two next scenarios.

5.2   DP with engine cost weight

A cost associated to the engine on/off is considered in this scenario. In a real vehicle the battery provides to the starter the amount of electrical energy needed to speed up the engine to the idle speed. After this point the engine combustion becomes stable and fuel can be injected in the cylinder to maintain the engine rotating.

The amount of energy consumed over an engine-off engine-on event, is given by

$$E_{on} = I_{batt}V_{batt}T_{on},$$

It is estimated[2] that, for the 6.7 L Diesel engine considered in our application, $E_{on} \sim 10$ kJ, which is equivalent to a battery state of charge variation of

$$\Delta SOC_{on} = \frac{E_{on}}{E_{batt}} = \frac{10 \text{ kJ}}{27 \text{ MJ}} \approx 0.37\%.$$

The DP algorithm was modified in order to account for the 'cost' associated to each engine-off engine-on which, in turn, increases the fuel economy by reducing the number of engine-on events. From a computational standpoint, the inclusion of a binary variable resulted in an increase of the execution time by a factor of two.

5.3 DP with clutch counter

To improve the drivability of the vehicle a clutch counter is implemented in the DP algorithm that reduces fast transients of the clutch. The timer was implemented in such a way the clutch is forced to stay in the same status (engaged or disengaged) for at least *n* seconds.

Since DP solves the optimisation problem backward in time, the implementation of a '*n*' second timer requires '*n*' additional binary state variables. The computational time of DP increases exponentially for each new state variable (e.g., '10' s clutch timer increases the computational time by a factor of 2^{10}). The clutch timer has been implemented for two seconds and four seconds corresponding to an increase in simulation time by a factor 4 and 16, respectively.

Each of the scenarios was analysed along six different driving cycles: Manhattan, WVU-sub, WVU-inter, APTA, HTUF, UDDS-truck to test the DP for urban, highway and mixed driving cycles. The code developed by Sundström and Guzzella (2009) was used to implement the three scenarios.

6 DP comparison under different driving scenarios

The comparison between the DP results has been done for the following configurations: no constraints, engine cost (10 kJ, 100 kJ) and clutch timer (2 s, 4 s). A summary of the overall results are shown in Table 2. As it can be noted, the driving mode selection does not seem to be clearly affected by the particular DP execution. The amount of time spent in each driving mode is very similar in all cases. The only qualitative difference is that the EV mode with engine ON is only used when the engine cost is considered. If no engine cost is considered at the time when the engine turns on, then there is no reason to keep the engine running with the only goal of providing power for the mechanical accessories.

Table 2   Driving mode selection statistics for different DP scenarios

	No constraint	Engine cost 10 kJ	Engine cost (10 kJ)	Clutch timer (2 s)	Clutch timer (4 s)
Parallel	43.63%	39.87%	42.42%	39.28%	39.24%
EV engine off	56.37%	59.77%	54.26%	60.72%	60.76%
EV engine on	0%	0.36%	3.31%	0%	0%
$\Delta SOC = SOC_{end} - SOC_{ref}$	0.000%	0.046%	0.234%	0.009%	0.160%

6.1   Near optimal rule-based strategy

The control based on a set of empirical rules is computationally efficient for an embedded CPU, but it can generate results which may be not optimal, if the vehicle is operating outside the domain where the rules were obtained.

Table 3 shows the frequencies for which the clutch transients and the engine ON/OFF events occur. Highest frequencies are obviously reached for the DP configuration with no constraint. Using an engine cost, it is possible to reduce the number of clutch transients by a factor 2.2. This factor does not change in the case of a higher cost (100 kJ). The events in which the engine turns ON are drastically reduced by a factor 3 and 7 for the engine cost of 10 kJ and 100 kJ, respectively. Despite of the DP configuration choice, the equivalent fuel consumption values (which take into account for the SOC variation at the end of the driving cycle) are very similar to the base-line set to the case of DP configuration with no constraints. As expected, the worst scenario is represented by the configuration with an engine cost of 100 kJ (+1.2% in comparison with the baseline).

Table 3   Average of clutch transients and engine on/off events along 6 different driving cycles; comparison of equivalent fuel consumption

	No constraint	*Engine cost (10 kJ)*	*Engine cost (10 kJ)*	*Clutch timer (2 s)*	*Clutch timer (4 s)*
Average number of clutch ON/OFF events in 1 s	0.085 s^{-1}	0.037 s^{-1}	0.038 s^{-1}	0.058 s^{-1}	0.040 s^{-1}
Average number of engine OFF/ON events in 1 s	0.085 s^{-1}	0.029 s^{-1}	0.012 s^{-1}	0.058 s^{-1}	0.040 s^{-1}
Equivalent fuel consumption	*100.0%*	*100.5%*	*101.2%*	*100.3%*	*100.5%*

In Figure 5 results from DP simulation with a clutch timer of 4 s are shown. The mode selection (Parallel and EV) information overlaps the velocity profile (composed by the concatenation of six different driving cycles).

Figure 5   (a) Driving cycle with driving mode selection and (b) optimal SOC profile from the DP simulations with a clutch timer of four seconds, (c) detail of driving mission and corresponding mode selection between 2,200 and 3,800 seconds and (d) actuators torque distribution (see online version for colours)
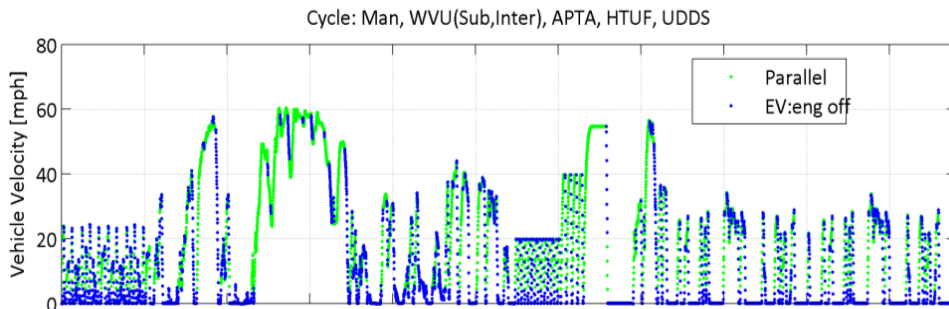
(a)

Figure 5 (a) driving cycle with driving mode selection and (b) optimal SOC profile from the DP simulations with a clutch timer of four seconds, (c) detail of driving mission and corresponding mode selection between 2,200 and 3,800 seconds and (d) actuators torque distribution (continued) (see online version for colours)

(b)

(c)

(d)
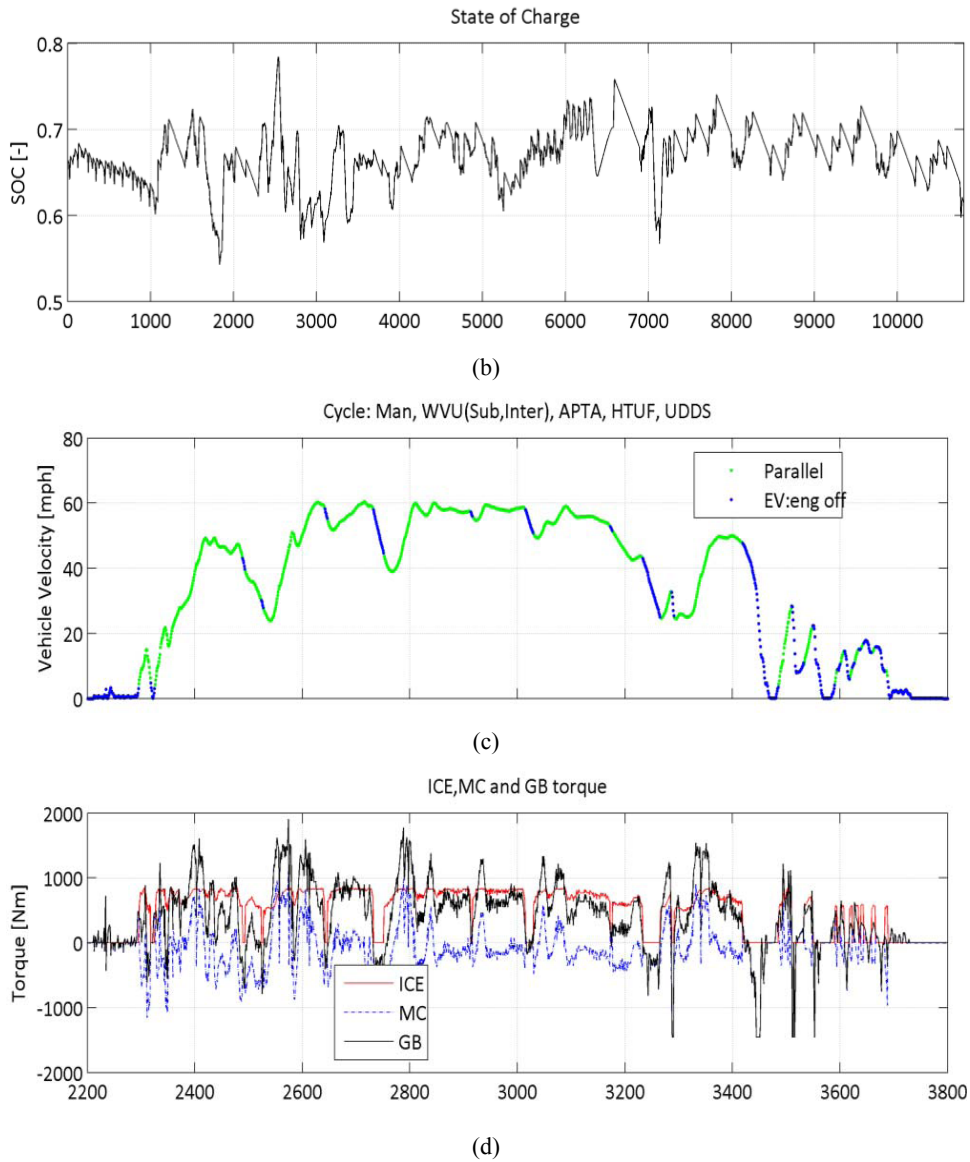
The constraint on the clutch switching makes the powertrain operating in a given mode ensuring better drivability. The SOC profile is shown at the bottom of Figure 5. The DP ensures an almost total usage of the SOC range by letting the SOC optimally vary within the admissible range (0.5–0.8).

7   Near optimal rule-based strategy

The control based on a set of empirical rules is computationally efficient for an embedded CPU, but it can generate results which may be not optimal, if the vehicle is operating outside the domain where the rules were obtained.

The calibration of a rule-based strategy, in addition, can also be not straightforward. The DP, on the other hand, provides the optimal solution on each driving cycle. In this section, the solution proposed by the DP (with an engine turn-on cost of 10 kJ) is analysed to extract rules that could reproduce the optimal behaviour. This approach, already known in literature, is applied in this work not only to determine the hybrid power split, but also to establish a 'nearly-optimal' powertrain mode of operation (some examples of this procedure are shown in Bianchi et al., 2011; Lin et al., 2003, 2004; Kum et al., 2010). Moreover, the rule-base strategy proposed in this paper can handle situations that can arise during real vehicle driving but which are not considered for the DP solution.

The starting point for deriving a rule-based strategy (RB) from DP is an extensive set of simulations in which the optimal driving strategy is found for several driving cycles and combinations of them, covering a wide range of urban and suburban driving conditions. The results are then studied and analysed in order to find common patterns and signal correlations, which are then replicated by suitable rules.

As mentioned in Section 3, the hybrid controller is configured in such a way that two layers are defined: the supervisory control module, which decides the best operating mode of the powertrain, and the energy management module, which is responsible for splitting the torque among the machines in order to satisfy the overall torque demand. This calls for the analysis of the DP strategy on two levels: mode selection (engine and clutch status) and torque split. The extraction of rules for each of these two levels is described the following sections.

Moreover, the design of the RB strategy is then completed and enriched with additional rules to account for situations that can arise in real vehicle operation.

7.1   Supervisory control module

The goal of the supervisory control module is to decide upon the powertrain configuration (clutch status and engine status) starting from the knowledge of the power requested by the driver, the gear number, the gearbox speed, the SOC and the temperatures of the powertrain components.

In normal conditions, the driving mode is selected from the distribution mode map in the plane 'total power demanded at the wheel vs. gearbox speed' as identified by the DP solution shown in Figure 6. The parallel mode (green points) is mostly chosen at speed higher than a certain threshold and positive power request, while the EV mode (engine off) is used during braking and vehicle launching (blue points).

In particular, in Figure 6 we can isolate three distinct areas in order to extract the following rules.

Area A   for engine speeds greater than the engine idle speed and for positive gearbox power, only the parallel configuration is chosen.

Area B   this area gathers points related to a negative power request, with clutch open ($C = 0$) and engine OFF.

Area C: at low speed and positive gearbox power, the powertrain works in pure electric (EV) mode, i.e., the clutch is open ($C = 0$) and the engine is OFF.

Figure 6   Powertrain mode selection from the DP solution (standard case with no constraints) over combinations of driving cycles (see online version for colours)
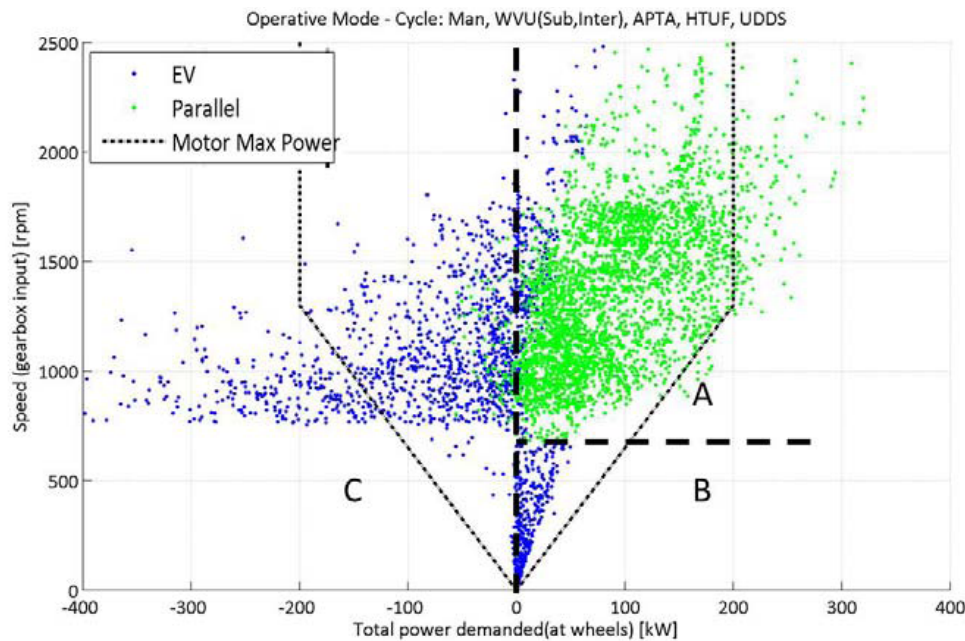
The design of the supervisory control module is performed starting from information in Figure 6 and completed by enforcing constraints on the clutch engaging/disengaging and engine on/off transitions to improve drivability. Moreover, the supervisory control module was implemented in order to address the 'exceptional'[3] situation of recharging the battery when the SOC is too low in case of vehicle at standstill.

7.1.1 Drivability constraints

To avoid repeated clutch and engine state variations, the RB strategy is implemented in such a way that a counter variable is introduced in the control algorithm which counts the seconds that the vehicle has spent in EV mode. The aim of the counter is both to improve the drivability by reducing transient of the clutch and to increase the fuel economy by reducing the number of engine ignition events. As seen in the DP simulations, a solution is to force the powertrain to be in EV mode for at least four seconds, unless the power requested is higher than the maximum electric power available and the gearbox speed is greater than the minimum speed of the engine. No constraints are considered to switch from parallel to EV mode, since for some kind of manoeuvres (e.g., fast start-stop) the

EV mode is required and the parallel mode cannot be maintained. In fact, the engine cannot run below a certain speed and it needs to be disconnected from the drivetrain when the vehicle approaches a stop.

7.1.2 Exception handling in RB strategy

When the vehicle is at standstill ($\omega_{wh} = 0$) and in EV mode, the electrical accessories are powered by the battery only. For the type of battery considered in our study it is estimated that the stored energy of the battery (starting form 0.65 SOC) can be depleted in less than 10 min, since:

$$\frac{E_{batt}\left(0.65 - SOC_{min}\right)}{P_{accelec}} = \frac{25 \ \text{MJ} \ (0.65 - 0.5)}{7 \ \text{kW}} \approx 578 \ \text{s} \ \approx 10 \ \text{min} \tag{18}$$

For this reason, a parallel driving mode in neutral gear is needed when the vehicle is at standstill for a long time (e.g., long queue) in order to recharge the battery without transmitting torque to the wheels. In fact, the only way to recharge the battery is turning ON the engine and disconnecting it from the wheels with the gearbox on neutral. This way the engine can supply mechanical power to the motor which works as a generator.

In reference to Figure 7, when the battery *SOC* reaches a threshold SOC_1, a flag called *Forcer* is set to 1. At this point, if the vehicle is standstill, the parallel mode with neutral gear is selected by the supervisory control module over the EV mode. This allows the battery *SOC* to increase (yellow area). When the *SOC* reaches a second threshold SOC_2, then *Forcer* is reset to 0. The SOC_1 and SOC_2 have been chosen equal to 0.60 and 0.70, respectively.

Figure 7   Qualitative representation of the 'exception' handled by the supervisory control module (see online version for colours)
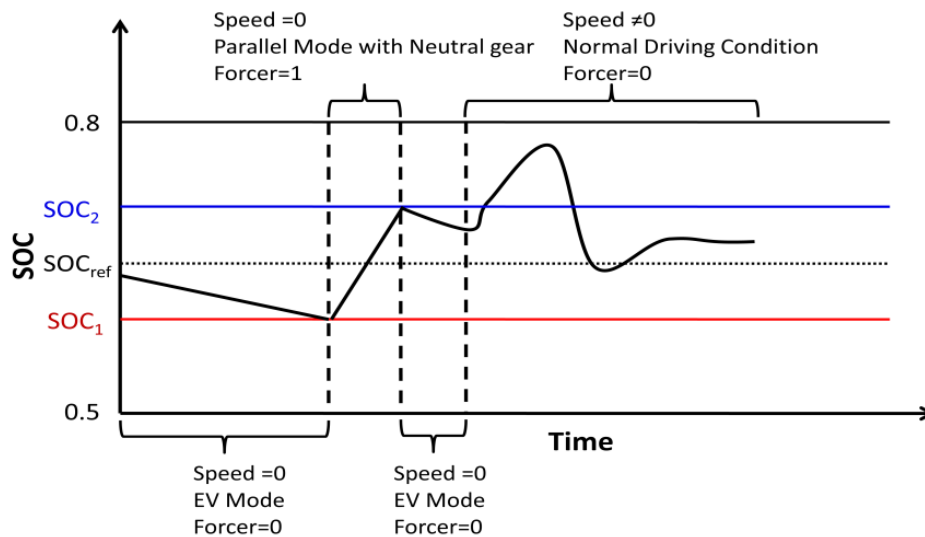
The supervisory control module has been implemented in the simplified model according to flowchart of Figure 8. The supervisory control module outputs the modes in which the powertrain will operate, which are:

- driving mode = 0 → electric mode

- driving mode = 1 → parallel mode

- driving mode = 2 → parallel mode with neutral gear.

The logic flow is articulated in such a way that, starting from the torque requested, the motor temperature is first checked and compared to a temperature threshold[4] ($Temp_1$ is given by the motor manufacturer) to ensure the motor is working within its limits.

Figure 8 Supervisory controller flowchart
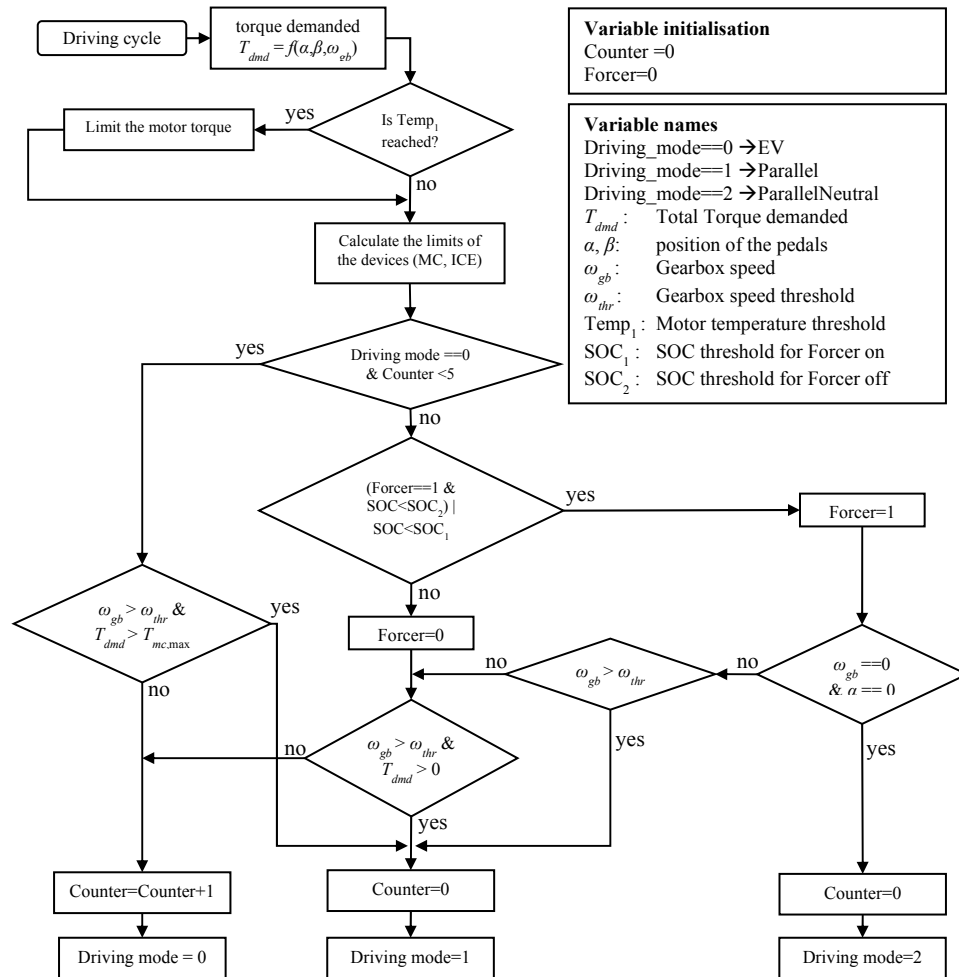
Then, if the vehicle is in EV mode and the variable *Counter* is lower than five seconds, the EV mode is selected (driving mode = 0) unless the power request is higher than the maximum capability of the EM alone, which require the use of the engine and the

selection of the parallel mode (driving mode = 1). In case none of these two modes is selected, the supervisor control module enforces the parallel mode with neutral gear after checking that the vehicle is at standstill and the variable *Forcer* is set to 1 when the *SOC* is below a threshold SOC_1 or if during the previous step the *Forcer* was already equal to 1. The variable *Forcer* is reset to 0 once the SOC becomes higher than SOC_2. The logic behind the variable *Counter* is needed to avoid frequent clutch engagements and disengagements; five seconds has been considered an appropriate value for the *Counter* threshold, in order to compromise the fuel consumption and the vehicle drivability.

7.2   Energy management module

The second layer of the hybrid controller is given by the energy management module, whose role is to choose the torque distribution between the EM, the engine and friction brakes based on the information provided by the supervisory control module and from the powertrain status. The information on driving mode, torque limitations and total torque demanded (from the supervisory control module) will enter the energy management module, in addition to the gearbox speed, the gear number, the SOC and the temperature of the motor (from the powertrain) according to the scheme in Figure 9. The energy management module processes this information and outputs the torque split. In the following, the strategy adopted for the torque split in the three modes is presented.

Figure 9   Energy management module
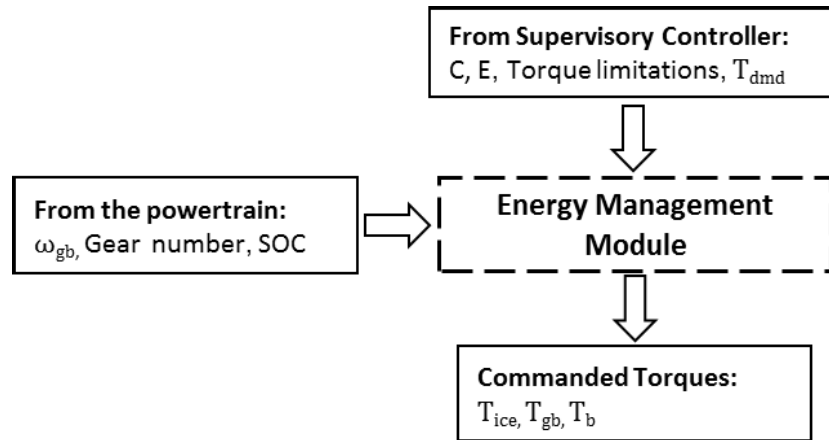
7.2.1 Torque distribution: EV mode

When the vehicle is in EV mode all the requested torque is provided by the EM. The friction braking is blended in only if the braking torque exceeds the motor availability.

7.2.2 Torque distribution: parallel mode with neutral gear

When the vehicle is in parallel mode and neutral gear, the target is to increase the SOC while keeping the powertrain working at its maximum efficiency point:

$$\max\left(\frac{\eta_{batt}\eta_{mc}\left(T_{ice}-T_{accmech}\right)\omega_{gb}-P_{accelec}}{\dot{m}_f Q_{lhv}}\right) \tag{19}$$

For the particular powertrain assumed in this study, the most efficient operating point occurs when (T_{ice}, ω_{ice}) = (841 Nm, 175 rad/s), as shown in Figure 10. This situation allows also a quick recharge of the battery, since it also corresponds to a relatively high power operating point.

Figure 10 Powertrain efficiency map and best operating point selected when the vehicle is in parallel mode with neutral gear (see online version for colours)
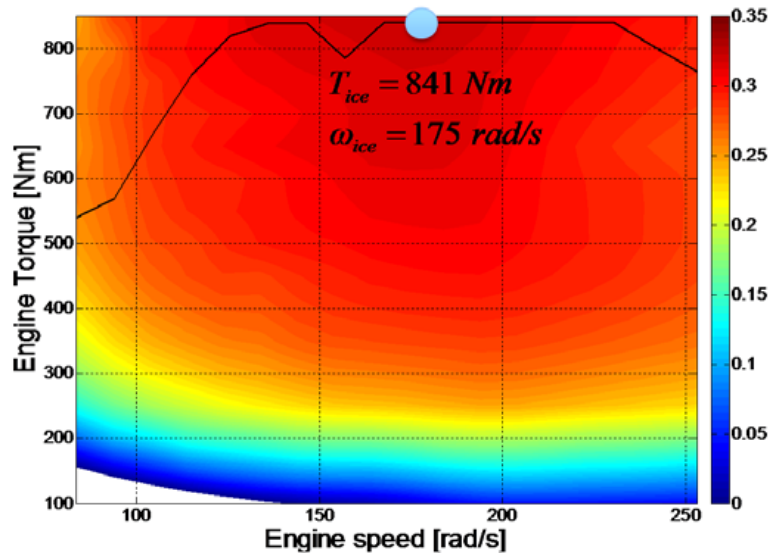
7.2.3 Torque distribution: parallel mode

When the vehicle is in parallel mode, the torque split between the EM and the engine is mostly a function of the total torque demanded. In fact, from the DP results shown in Figure 11, a linear function seems to well approximate the relation between T_{MC} and T_{gb}. The linear function

$$T_{MC} = mT_{dmd} + k \tag{20}$$

is used next as a splitting rule in the energy management module in parallel mode.

7.2.3.1 Calibration of torque distribution law in parallel mode

The correlation and linear fitting in Figure 11 does not carry any dependence of the torque split on the actual SOC of operation. This information, on the other hand, is crucial in order to enforce and guarantee the operation within battery limitations.

The intuitive idea is to promote the use of electric power for traction at high SOC values. On the other hand, the use of the EM as a generator is preferred when the SOC is low. This corresponds to shift up and down the torque split line as a function of *SOC*.

One way of doing so is by means of modifying equation (21) to include an extra term, a penalty function p, whose role is to account for SOC in the linear torque split:

$$T_{MC} = mT_{dmd} + kp. \tag{21}$$

A feedback from the SOC mechanism is implemented, through a penalty function, to monitor the behaviour of the SOC to avoid unexpected deviation from the charge-sustaining value (set to 0.68%). The penalty function will provide a small correction for small deviation from the SOC reference and more important corrections when the deviation becomes more pronounced.

Figure 11   Linear fit of the torque split distribution in parallel mode (see online version for colours)
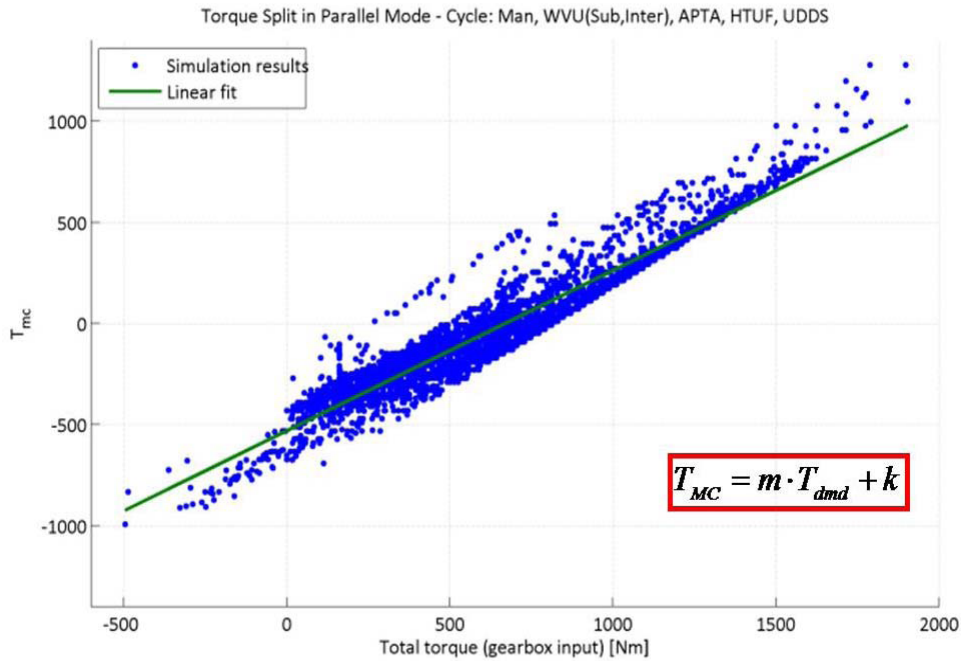
The penalty function selected is:

$$p = -\mu \cdot x_{SOC}^{n} + 1, \tag{22}$$

where x_{SOC} measures the distance of the *SOC* from a reference value SOC_{μ} and it is defined as:

$$x_{SOC} = \frac{SOC - SOC_{\mu}}{\dfrac{SOC_{max} + SOC_{min}}{2}} \tag{23}$$

where

μ defines the gain of the penalty function depending on how far the SOC is from SOC_μ, in particular μ will assume two distinct values corresponding to the two cases when SOC is higher or lower than SOC_μ.

n is the exponent of the penalty function which defines the degree of the polynomial function. The higher the value of n, the higher the correction when the *SOC* is deviating from SOC_μ. The value chosen in this study is $n = 3$.

SOC_μ is the parameter that has to be tuned in order to have an acceptable SOC profile for given driving cycles, to avoid to discharge/recharge the battery over the limits and to minimise the equivalent fuel consumption. Intuitively, high values for SOC_μ will tent to position the actual SOC at high value as well which can result in a limitation of the regenerative braking capability with a negative impact on fuel consumption. On the other hand, low values for SOC_μ might result in frequent condition of low SOC: this may prevent from having enough electrical power available to perform an efficient torque split behaviour or either to satisfy the overall power request from the driver.

The calibration of equations (22) and (23), in terms of selection of best values of μ is conducted considering two scenarios: when $SOC = SOC_{max}$ and when $SOC = SOC_{min}$.

When $SOC = SOC_{max}$ and the torque demanded, T_{dmd}, is zero, the motor should not recharge the battery and should not provide a positive torque, i.e., $T_{mc} = 0$ (otherwise it should be braked by the ICE or by the friction brakes). Thus, from equation (21) we obtain:

$$mT_{dmd} + pk = T_{mc} \rightarrow p = 0, \quad \text{for} \quad SOC = SOC_{max} \tag{24}$$

This implies that

$$1 - \mu_1 x_{SOC}^n = 0 \rightarrow \mu_1 = \frac{-1}{x_{SOC}^n}. \tag{25}$$

This means that when the *SOC* is higher than the SOC_μ, the linear split gradually shifts up until the penalty function becomes zero, for $SOC = SOC_{max}$.

When $SOC = SOC_{min}$, the EM has to at least provide the battery with enough power to sustain the electrical accessories. Thus, the maximum motor torque requested, at minimum gearbox speed is:

$$T_{accelec,max} = \frac{P_{accelec}}{\omega_{gb}\eta_{em}\left(\omega_{gb,thr}, T_{accelec}\right)} = 130 \ \text{Nm}. \tag{26}$$

The maximum value of the demanded torque is then:

$$T_{dmd,max} = T_{ice,max} - T_{accelec,max} \leq (841 - 130) \ \text{Nm} = 711 \ \text{Nm} \tag{27}$$

Hence, at $SOC = SOC_{min}$, equation (22) becomes:

$$mT_{dmd} + kp = T_{mc} \rightarrow mT_{dmd,max} + kp = -T_{accelec,max}, \tag{28}$$

which gives:

$$\mu_2 = \frac{1 + \dfrac{mT_{dmd,max} + T_{accelec,max}}{k}}{x_{SOC}^n} \tag{29}$$

When the SOC is lower than the SOC_μ (Figure 12), the linear split gradually shifts down until the penalty function becomes:

$$p = -\frac{T_{accelec,max} + T_{dmd,max}}{k} \tag{30}$$

The two values found for μ, i.e., μ_1 and μ_2, are then used to force the SOC to be remain close to the SOC_μ. Closer the SOC value is to SOC_{max} or SOC_{min}, stronger is the penalty function effect. The penalty function effect is null ($p = 1$) when $SOC = SOC_\mu$.

Figure 12   Split function shift when the SOC is lower than SOC_μ (see online version for colours)
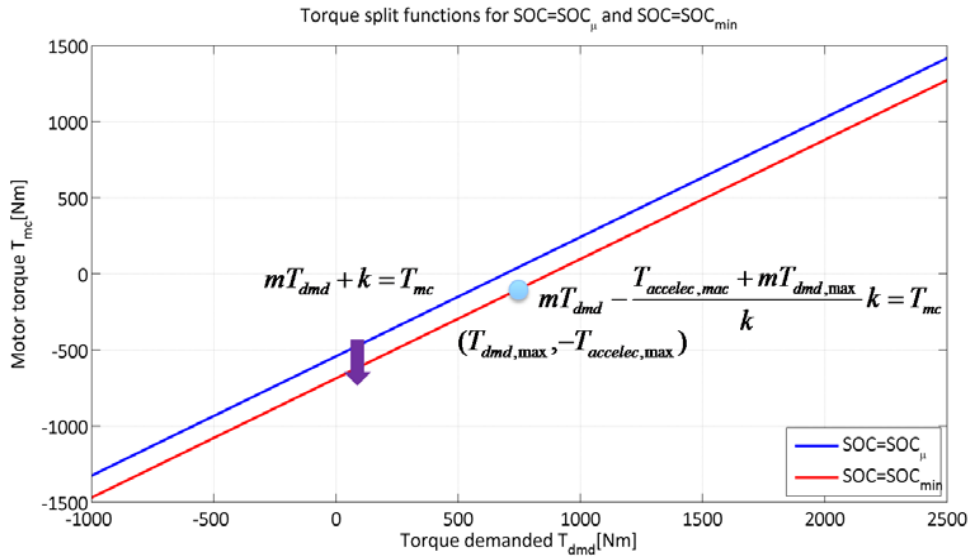
7.2.3.2   Calibration of SOC_μ

SOC_μ is the second parameter to calibrate in equation (22). Moving SOC_μ between the maximum and minimum acceptable values for SOC, i.e., 0.8 and 0.5, Has an effect on shape of the penalty function. In general, for low value of SOC_μ the control strategy reacts stronger to value of $SOC > SOC_\mu$, while if SOC_μ is high, the penalty weight is larger for $SOC < SOC_\mu$.

Simulations are performed in order to test the behaviour of the RB strategy for six different driving cycles: Manhattan, APTA, WVU-sub, WVU-inter, HTUF and UDDS-Truck. Each driving cycle has also been also considered three consecutive times to test the steady state behaviour of the SOC profile. Moreover, the RB strategy was tested for five different values of the tuning parameter SOC_μ (0.55, 0.60, 0.65, 0.70, and 0.75) in order to select the suitable value of SOC_μ. Values of μ_1 and μ_2 are reported in Table 4 for different choices of SOC_μ.

Table 4 Calibrated μ_1 and μ_2 for different values of SOC_μ

SOC_μ	μ_1	μ_2
0.55	0.074	9.83
0.60	0.90	3.38
0.65	1	0.26
0.70	0.42	0.11
0.75	0.22	0.058

From Figures 13 and 14 the general trend is that for high SOC_μ, the SOC profile tends to be more charge increasing, (in some cases the SOC can reach the maximum SOC threshold which then can limit the regenerative braking capability) while for low SOC_μ, the battery SOC tends to be more charge depleting.

The RB strategy has been applied to a model that considers an engine start cost of 10 kJ; analogously, the results have are benchmarked against the DP solution that considers the same engine cost. Overall, the RB strategy satisfactorily mimics the DP behaviour. However, a noticeable difference is that the RB strategy does not have any constraint that forces the final value of SOC to be equal to the initial SOC value, which is why the difference between the final SOC from RB and from DP can be elevated, as shown in Figures 13 and 14.

Figure 13 Comparison of SOC profiles generated from the DP and for the rule-based strategy along the UDDS-Truck driving cycle (see online version for colours)
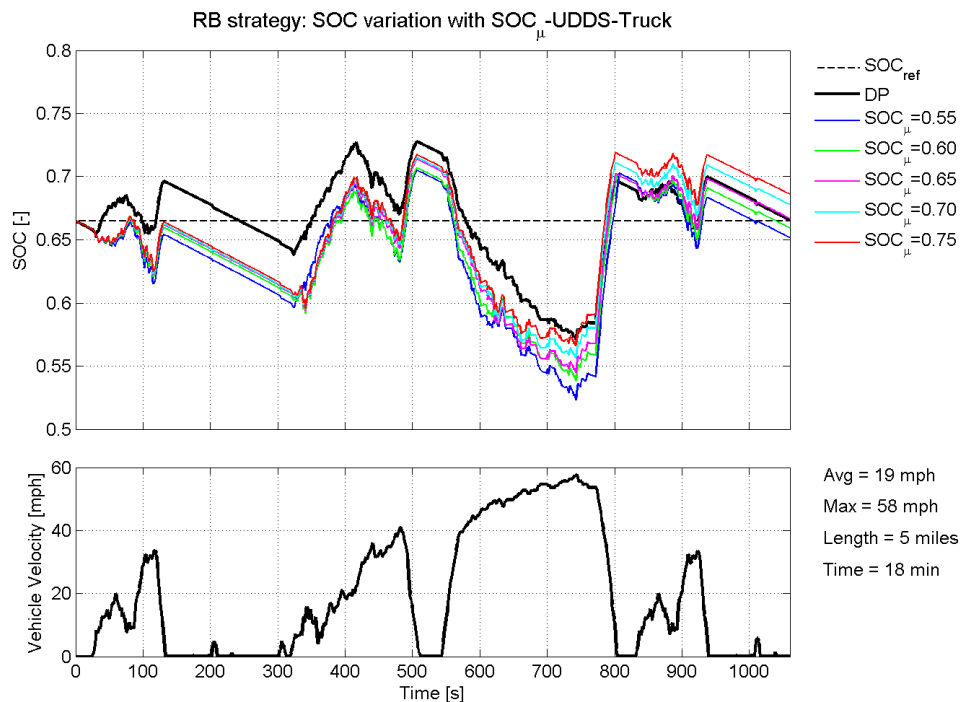
Figure 14   Comparison of SOC profiles generated from the DP and for the rule-based strategy along the HTUF driving cycle (see online version for colours)
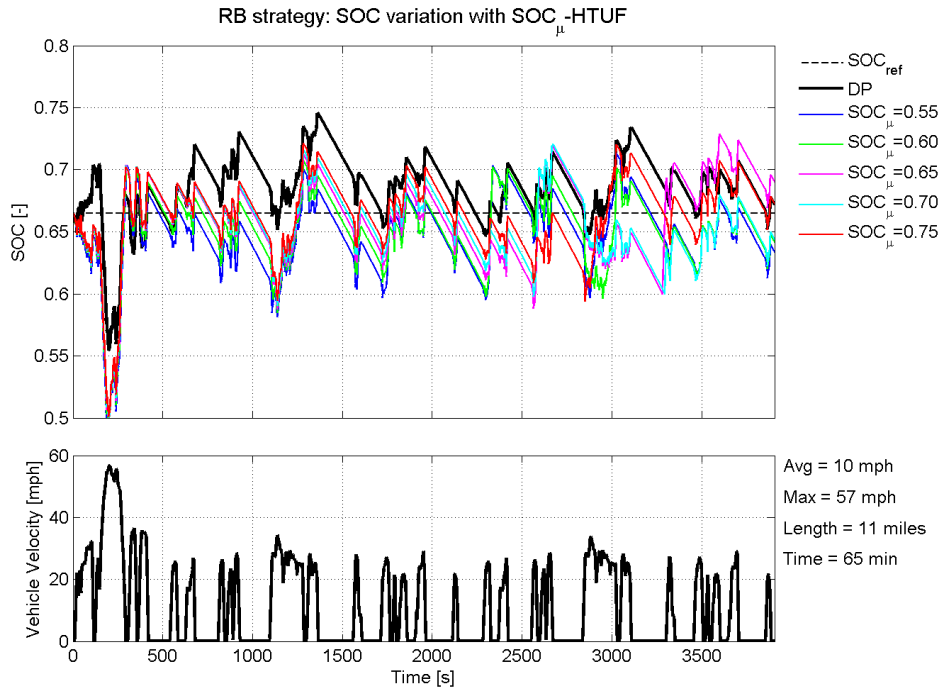
However, the behaviour of the two profiles is very similar. The results on equivalent fuel consumption reported in Table 5 confirm this: the RB strategy is within 2% of increase of fuel consumed as compared with the optimal DP results. From the simulation study, we selected a value of 0.70 to calibrate SOC_μ. This value ensures that:

- the torque requested by the driver is satisfied for all the driving cycles

- the equivalent fuel consumption is not significantly different in comparison with the other tuning choices.

Table 5   Comparison of equivalent fuel consumption for different values of SOC_μ generated six different driving cycles

SOC_μ	TOTAL ΔFC_{eqv} (%)
$SOC_\mu = 0.55$	1.30
$SOC_\mu = 0.60$	1.44
$SOC_\mu = 0.65$	1.51
$SOC_\mu = 0.70$	1.43
$SOC_\mu = 0.75$	1.57

An improvement in the overall drivability obtained with the RB design can be observed in Figure 15 when compared to Figure 5 as repeated engine on/off switching and clutch engagement/disengagement are now absent as they have been explicitly accounted for in the RB design.

Figure 15 (a) Driving cycle with driving mode selection and (b) SOC profile from the RB
simulations with a clutch timer of four seconds; (c) detail of driving mission and
corresponding mode selection between 2,200 and 3,800 seconds and
(d) actuators torque distribution (see online version for colours)

(a)

(b)

(c)

(d)
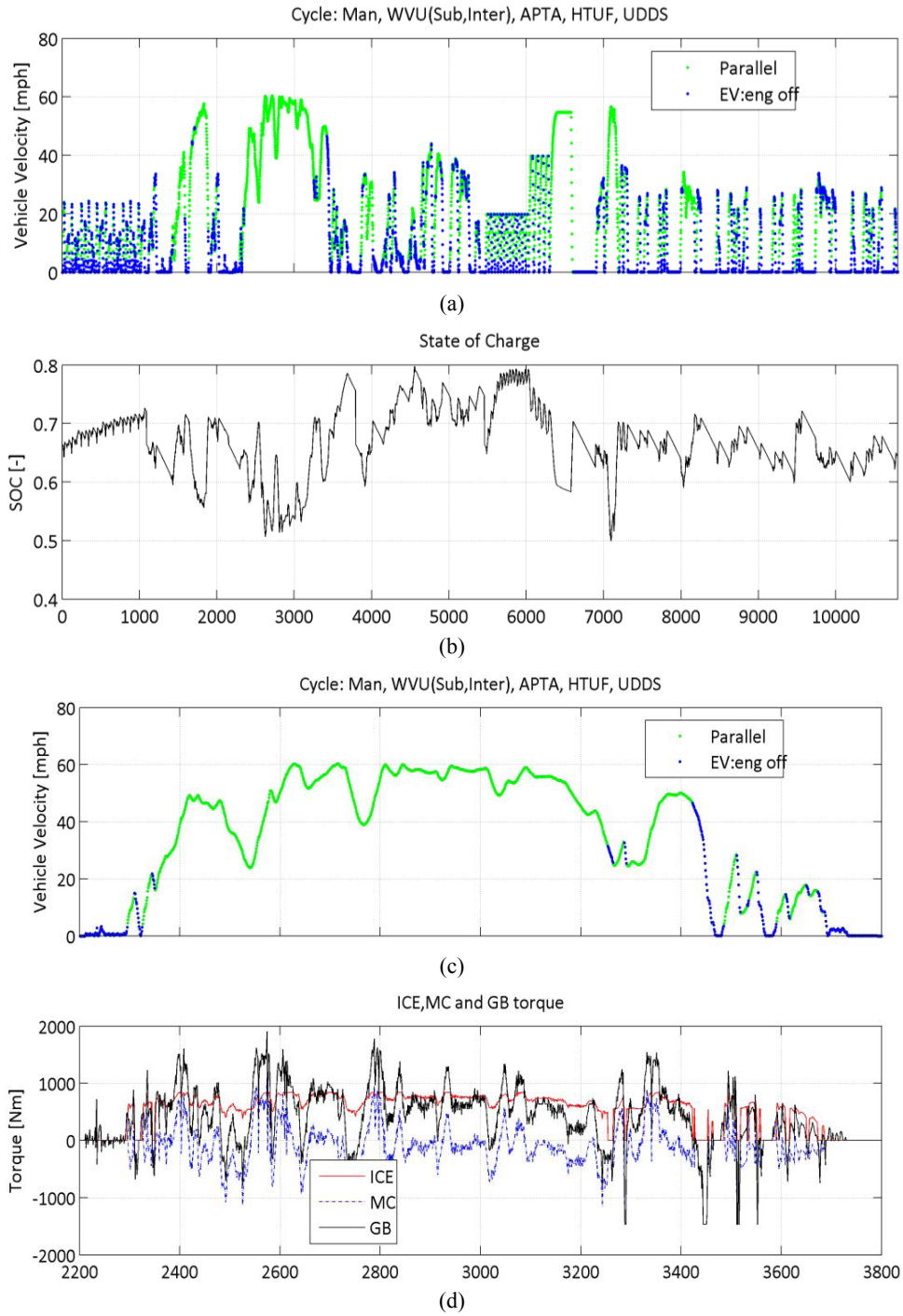
8   Conclusions

In this paper we have proposed the design of an energy management strategy for medium duty hybrid truck by extracting rules from the DP algorithm. The proposed rule-based strategy has the clear advantage of being near-optimal, easy to implement on-board of the vehicle, computationally cheap, with low calibration load and systematic. By analysing the DP results, the two-layer rule-based control strategy has been tuned to minimise the fuel consumption and ensure satisfactory drivability.

References

Ayalew, B. and Molla, S.K. (2011) 'Power management strategies for a series hydraulic hybrid drivetrain', *Int. J. Powertrains*, Vol. 1, No. 1, pp.93–116.

Bianchi, D., Rolando, L., Serrao, L., Onori, S., Rizzoni, G., Al-Khayat, N., Hsieh, T.T.M. and Kang, P. (2011) 'Layered control strategies for hybrid electric vehicles based on optimal control', *International Journal of Electric and Hybrid Vehicles*, Vol. 3, No. 2, pp.191–217.

Brahma, A., Guezennec, Y. and Rizzoni, G. (2000) 'Optimal energy management in series hybrid electric vehicles', in *2000 American Control Conference*.

Cipollone, R. and Sciarretta, A. (2006) 'Analysis of the potential performance of a combined hybrid vehicle with optimal supervisory control', in *Proceedings of the 2006 IEEE International Conference on Control Applications*.

Jalil, N., Kheir, N. and Salman, M. (1997) 'A rule-based energy management strategy for a series hybrid vehicle', *Proceedings'*.

Kum, D., Peng, H. and Bucknor, N. (2010) 'Optimal control of the plug-in HEV for fuel economy under various travel distances', in *6th IFAC Symposium on Advances in Automotive Control*, Munich, Germany.

Lewis, F. and Syrmos, V. (1995) *Optimal Control*, Wiley-Interscience, New York.

Lin, C., Filipi, Z., Louca, L., Peng, H., Assanis, D. and Stein, J. (2004) 'Modelling and control of a medium-duty hybrid electric truck', *International Journal of Heavy Vehicle Systems*, Vol. 11, Nos. 3–4, pp.349–371.

Lin, C., Peng, H., Grizzle, J.W. and Kang, J. (2003) 'Power management strategy for a parallel hybrid electric truck', *IEEE Transactions on Control Systems Technology*, November, Vol. 11, No. 6, pp.839–849.

Musardo, C., Rizzoni, G., Guezennec, Y. and Staccia, B. (2005) 'A-ECMS: an adaptive algorithm for hybrid electric vehicle energy management', *European Journal of Control*, Vol. 11, Nos. 4–5, pp.509–524.

Paganelli, G., Brahma, A., Guezennec, Y. and Ercole, G. (2001) 'General supervisory control policy for the energy optimization of charge-sustaining hybrid electric vehicles', *JSAE Review*, Vol. 22, No. 4, pp.511–518.

Piccolo, A., Ippolito, L., Galdi, V. and Vaccaro, A. (2001) 'Optimization of energy flow management in hybrid electric vehicles via genetic algorithms', in *Proceedings of the 2001 IEEE/ASME International Conference on Advanced Intelligent Mechatronics*, Como, Italy.

Salman, M., Schouten, N. and Kheir, N. (2000) 'Control strategies for parallel hybrid', in *American Control Conference*.

Sciarretta, A. and Guzzella, L. (2007) 'Control of hybrid electric vehicle', *IEEE Control Systems Magazine*, pp.60–70.

Sendur, P., Stein, J., Peng, H. and Louca, L. (2003) 'An algorithm for the selection of physical system model order based on desired state accuracy and computational efficiency', in *Proceedings of the 2003 ASME International Mechanical Engineering Congress and Exposition*.

Serrao, L., Onori, S. and Rizzoni, G. (2011) 'A comparative analysis of energy management strategies for hybrid electric vehicles', *ASME Journal of Dynamic Systems, Measurement and Control*, Vol. 133, No. 3, pp.1–9.

Sundström, O. and Guzzella, L. (2009) 'A generic dynamic programming Matlab function', in *18th IEEE International Conference on Control Applications*.

Notes

1 Since 1999, Argonne national Laboratories undertook a collaborative effort to further develop the Powertrain System Analysis Toolkit © (PSAT) under the direction of and with contributions from Ford, General Motors, and DaimlerChrysler. Sponsored by the U.S. Department of Energy (DOE), the software has become widely accepted by industry and has been licensed to more than 130 companies, universities, and research laboratories worldwide with more than 750 users.

2 The amount of energy requested to turn on the engine varies with the engine temperature. However, here a rough estimate of the amount of energy needed when the engine is already warmed up (turn on during driving) is given, based on the assumption that the amount of energy, E_{on}, required to turn on a 2.0 L diesel engine on a conventional car is approximately 2.8 kJ (given a voltage of 14 V for the PbA and a current of about 200 A).

3 This case was not modelled in the DP scenarios and because of this is called 'exceptional'.

4 Some of the powertrain components, such as the EMs and generators, may limit their powertrain capability when they exceed a given temperature. If this happens, then the control strategy has to limit the power or the torque that can be requested in order to avoid the component failure.

List of symbols

Variable	Units	Description
A	m^2	Vehicle frontal area
α	rad	Road slope
C	-	Clutch status engaged/disengaged
c_0	-	Constant term of the rolling resistance polynomial
c_1	s/m	Linear term of the rolling resistance polynomial
c_2	s^2/m^2	Square term of the rolling resistance polynomial
c_3	s^3/m^3	Cubic term of the rolling resistance polynomial
C_d	-	Coefficient of aerodynamic drag
c_r	-	Coefficient of rolling resistance
E	-	Engine status ON/OFF
E_{batt}	J	Battery energy capacity
E_{on}	J	Electrical energy needed to turn on the engine
η_{batt}	-	Battery efficiency
η_d	-	Differential efficiency
η_{mc}	-	Electric motor efficiency
η_{ice}	-	Engine efficiency
η_{gb}	-	Transmission efficiency

List of symbols (continued)

Variable	Units	Description
F_a	N	Aerodynamic resistance
F_g	N	Grade force
F_r	N	Rolling resistance
F_w	N	Tractive force produced at the wheels
g	m/s^2	Acceleration of gravity
I	A	Battery current
J_{ice}	kg*m^2	Engine rotational inertia
J_w	kg*m^2	Wheel rotational inertia
k	N*m	Constant term of the first order polynomial curve fit for the torque split of the rule-based strategy (without penalty function)
M	kg	Vehicle mass
m	-	Linear term of the first order polynomial curve fit for the torque split of the rule-based strategy
M_{eq}	kg	Equivalent vehicle mass including the equivalent drivetrain inertia
$\dot{m}_{elec}$	kg/s	Virtual instantaneous fuel consumption equivalent to the electrical energy used
$\dot{m}_f$	kg/s	Instantaneous fuel consumption
μ	-	Penalty function gain for the torque split rule-based strategy
μ_1	-	Penalty function gain for the torque split rule-based strategy This is adopted when $SOC > SOC_\mu$
μ_2	-	Penalty function gain for the torque split rule-based strategy This is adopted when $SOC < SOC_\mu$
n	-	Exponent value of the penalty function for the torque split rule-based strategy
p	-	Penalty function for the torque split rule-based strategy
$P_{accelec}$	W	Power request by the electrical auxiliary loads
$P_{accmech}$	W	Power request by the mechanical auxiliary loads
P_{batt}	W	Battery power
P_{fuel}	W	Chemical fuel power
P_{ice}	W	Engine mechanical output power
$P_{mc,e}$	W	Electrical power absorbed by the electric motor
Q_{batt}	Ah	Battery charge
$Q_{batt,max}$	Ah	Maximum charge capacity of the battery
Q_{lhv}	J/kg	Fuel lower heating value
R	m	Tire rolling radius
ρ_{air}	kg/m^3	Air density
SOC	-	Battery state of charge
SOC_μ	-	SOC reference value in the rule-based strategy
τ_d	-	Differential gear ratio

List of symbols (continued)

Variable	Units	Description
τ_{gb}	-	Gearbox ratio
t	s	Time
$T_{accelec}$	Nm	Torque needed to provide enough power for the electrical accessories without discharging the battery
$T_{accelec,max}$	Nm	Maximum torque needed to provide enough power for the electrical accessories without discharging the battery
$T_{accmech}$	Nm	Torque absorbed by the mechanical accessories
T_b	Nm	Friction brake torque
T_{dmd}	Nm	Torque demand at the wheels
$T_{dmd,max}$	Nm	Instantaneous maximum torque that can be demanded at the wheels, given the limitations of the components
T_{gb}	Nm	Torque at the gearbox input shaft (produced by the powertrain)
T_{ice}	Nm	Engine torque
$T_{ice,min}$	Nm	Minimum engine torque for a given rotational speed
T_{mc}	Nm	Electric motor torque
$T_{mc,min}$	Nm	Minimum electric motor torque for a given rotational speed
T_w	Nm	Torque at the wheel (produced by the powertrain
V	m/s	Vehicle speed
V_{batt}	V	Battery voltage
ω_{ice}	rad/s	Engine rotational speed
ω_{idl}	rad/s	Engine idle rotational speed
ω_{gb}	rad/s	Gearbox input shaft speed
$\omega_{gb,thr}$	rad/s	Minimum engine shaft speed for the engine to be coupled with the gearbox input shaft
ω_{mc}	rad/s	Electric motor rotational speed
ω_w	rad/s	Wheel rotational speed
x_{SOC}	-	Measure of the SOC distance from a reference value SOC_μ